nomial smoothing system is shown to be adequate in altitude determination accuracy, but marginal in velocity accuracy, for an earth orbital rendezvous mission. On the other hand, this system may be adequate for a lunar landing mission depending upon the characteristics of the lunar parking orbit. The performance of the exact smoothing scheme is shown to be more than adequate for both of these missions. However, the exact smoothing system is more complicated than the polynomial system. Whether or not this complication is justified by the improved results depends upon mission requirements of the vehicle.

Comparative position and velocity errors for the exact least squares fit and a third-order polynomial approximation are presented in Table 7. The smoothing times were chosen to be the optimal smoothing times for the polynomial, considering the data accuracy and rate, and the truncation errors to be expected. It is seen that the exact fit gives uniformly smaller errors and that the improvement in position error may be a factor of two or more, whereas that in velocity may be an order of magnitude. For shorter somoothing times the errors would be more nearly comparable. On the other hand, for longer smoothing times the errors for the polynomial approximation would increase, whereas those for the exact fit would continue to decrease rapidly. It is particularly instructive to compare the first and third columns in Table 7. Here the only difference is the data rate, one sample per second in the first case and one sample every 10 sec in the second. It is seen that the error from the exact fit at the low data rate is generally less than the error from the polynomial approximation at the higher data rate. Hence, the apparent complexity of the exact fit is not a measure of the total number of arithmetic operations to be performed. This may actually be reduced for the same accuracy. Nevertheless, exact fitting requires a digital computer whereas polynomial smoothing only requires a relatively simple digital differential analyzer. If a digital computer must be carried for other parts of the overall mission, its capacities may be put to good use in performing a least squares fit using the exact model. Thus, if the satellite navigation system uses an inherently exact smoothing scheme, instrumentation requirements may be relaxed.

References

1 "Rendezvous guidance and mechanization for orbital launch operations," Raytheon Co. Rept. BR-1469B (December 20, 1961); unclassified.

2 Duke, W., "Lunar landing problems," Lunar Flight Symposium, Am. Astronaut. Soc. Denver, Colo. (December 29, 1961).

3 Lunde, B., "Horizon sensing for attitude determination," Goddard Memorial Symposium, Am. Astronaut. Soc. Preprint 62–47 (March 1962).

4 Worsmer, E. and Arck, M., "Infrared navigation sensors for space vehicles," ARS Preprint 1928–61 (1961).

5 Kendall, P. and Stalcup, R., "Attitude reference devices for space vehicles," Proc. Inst. Radio Engrs. **48**, 765–770 (April 1960).

6 "All altitude horizon sensors," Barnes Engineering Co. Special Sheet 13-160 (April 15, 1961).

7 Kovit, B., "IR horizon sensor guides planetary orbiting," Space/Aeronaut. **35**, 131–133 (February 1961).

8 "Lunar landing," Raytheon Co. Rept. BR-1394 (October 20, 1961); unclassified.

9 Nesline, F. W., Jr., "Polynomial filtering of signals," Inst. Radio Engrs. Trans. Military Elecron. pp. 531–542 (June 1961).

10 Satyendra, K. N. and Bradford, R. E., "Self-contained navigational system for determination of orbital elements of a satellite," ARS J. **31**, 949–956 (1961).

OCTOBER 1963 AIAA JOURNAL VOL. 1, NO. 10

Buckling of a Truncated Hemisphere under Axial Tension

JOHN C. YAO*

Northrop Norair, Hawthorne, Calif.

This report is concerned with the theoretical evaluation of the buckling strength of a truncated hemisphere under axial tensile load. The edges of the shell are assumed to be restrained from moving radially or from rotating. Theoretical results were obtained by Vlasov's small deflection theory and Galerkin's method. The quick convergence of the series solution is demonstrated. Comparison of theoretical values with a few available experimental results is given.

Nomenclature

A_n, B_n	= coefficients of series expansion for radial deflection and stress function, respectively
a	= mean radius (see Fig. 2)
E	= Young's modulus
l	= $\sin\alpha$
m	= number of buckle waves in the circumferential direction
P	= axial tensile load per unit circumferential length at the shell equator
q	= radial load per unit middle surface area
$T_\phi, T_\theta, T_{\phi\theta}, T_{\phi\theta}$	= additional force components in the buckled shell
$T_{\phi 0}, T_{\theta 0}$	= membrane force components prior to buckling
t	= shell thickness
w	= radial buckling displacement of a middle surface point
x	= $\sin\phi$
α	= altitude angle of the truncated edge (see Fig. 2)
θ,ϕ	= spherical coordinates (see Fig. 2)
μ	= Poisson's ratio
Φ	= stress function
∇^2	= Laplace's operator $[(\partial^2/a^2\partial\phi^2) - \tan\phi(\partial/a^2\partial\phi) + \sec^2\phi(\partial^2/a^2\partial\theta^2)]$

Received January 25, 1963; revision received June 21, 1963. The author wishes to take this opportunity to thank A. J. Carah, Chief Engineer, Missile Systems, Douglas Aircraft Company Inc., for permission to publish the testing results; he also wishes to thank his supervisor, P. Seide, for invaluable comments and suggestions. The assistance of J. Yamane in checking the algebra and of J. Riley and G. Johnson for programming support also is acknowledged.

* Senior Scientist.

I. Introduction

A TRUNCATED hemisphere may buckle under an axial tensile load that exceeds a certain critical value (Fig. 1) because of compressive hoop stresses. The buckled shape is similar to that of a cylinder buckled under radial pressure, with one half-wave in the axial direction and many small waves in the circumferential direction. The present theoretical study treats the case where both the truncated edge and the edge at the equator are restrained from moving radially or from rotating.

In the analytic work, Vlasov's equations of equilibrium and compatibility condition[1] are used. These equations are satisfied by the use of Galerkin's method[2] in conjunction with expressions for the radial displacement and the stress functions that satisfy the approximate boundary conditions.

Numerical results of theoretical buckling loads for shells of various geometric configurations are given by curves as well as by simplified algebraic formulas and are compared with a few experimental data.

II. Theory

Using spherical coordinate system ϕ and θ, as shown in Fig. 2, the equilibrium condition in the radial direction for a spherical shell element can be expressed by the following equation:

$$\frac{1}{12\,(1-\mu^2)}\left(\frac{t}{a}\right)^2 a^4\nabla^4\left(\frac{w}{a}\right) - a^2\nabla^2\left(\frac{\Phi}{Ea^2t}\right) - \frac{aq}{tE} = 0 \quad (1)$$

where

$$a^2\nabla^2 = (\partial^2/\partial\phi^2) - \tan\phi\,(\partial/\partial\phi) + \sec^2\phi\,(\partial^2/\partial\theta^2)$$

$$\nabla^4 = \nabla^2\nabla^2$$

and Φ is the stress function, in terms of which the additional force components in the buckled shell wall are given by

$$T_\phi = -\frac{1}{a^2}\left(\sec^2\phi\,\frac{\partial^2\theta}{\partial\Phi^2} - \tan\,\frac{\partial\Phi}{\partial\phi}\right)$$

$$T_\theta = -\frac{1}{a^2}\frac{\partial^2\Phi}{\partial\phi^2} \quad (2)$$

$$T_{\phi\theta} = T_{\phi\theta} = \frac{1}{a^2}\sec\phi\left(\frac{\partial^2\Phi}{\partial\phi\partial\theta} + \tan\phi\,\frac{\partial\Phi}{\partial\theta}\right)$$

Equations (2) approximately satisfy the equations of equilibrium for a shell element in both the meridional and the circumferential directions. The stress function Φ and the radial deflection w also are related by the compatibility equation:

$$a^4\nabla^4\,(\Phi/Ea^2t) + a^2\nabla^2\,(w/a) = 0 \quad (3)$$

Equations (1) and (3) are Vlasov's equations,[1] expressed in spherical coordinates.

In dealing with the problem of stability of a spherical shell, one must take into account the radial component of stress existing prior to buckling. With the assumption that these prebuckling stresses are represented adequately by the membrane state of stress, one has

$$T_{\phi 0} = -T_{\theta 0} = P\sec^2\phi \quad (4)$$

During buckling, because of curvature changes, these finite membrane forces contribute a radial component equal to

$$q = \frac{P}{a^2}\left(\frac{\partial^2 w}{\partial\phi^2} - \sec^2\phi\,\frac{\partial^2 w}{\partial\theta^2} + \tan\phi\,\frac{\partial w}{\partial\phi}\right)\sec^2\phi \quad (5)$$

which is used in Eq. (1).

The boundary conditions chosen to be satisfied by the radial deflection w and the stress function Φ are those corresponding to shell edges that are restrained from moving radially or from rotating, motion in the meridional and circumferential directions being restrained insofar as rigid body motion is concerned. These conditions may be expressed as

$$w = \partial w/\partial\phi = T_\phi = T_{\phi\theta} = 0 \qquad \text{at } \phi = 0,\ \alpha \quad (6a)$$

or, for Eq. (2), as

$$w = \partial w/\partial\phi = \Phi = \partial\Phi/\partial\phi = 0 \qquad \text{at } \phi = 0,\ \alpha \quad (6b)$$

A possible method of solving the problem would be first to assume an arbitrary radial deflection function that satisfies the radial deflection boundary conditions (6); then Eq. (3) could be solved for the stress function Φ in terms of a particular solution involving w and the general solution of the homogeneous equation, the constants of integration being determined by the stress function boundary conditions. Finally, the radial deflection function and the derived stress function can be substituted into Eq. (1), which then could be solved by means of the Galerkin method.[2] Because it is difficult to solve for the stress function in terms of the radial deflection function, however, this method of solution can be replaced by the equivalent process of choosing arbitrary functions that satisfy the appropriate boundary conditions for both the stress function Φ and the radial deflection function w and solving both Eqs. (1) and (3) by the Galerkin method. Thus,

$$\int_0^\alpha\int_0^{2\pi}\left[\frac{1}{12\,(1-\mu^2)}\left(\frac{t}{a}\right)^2 a^4\nabla^4\left(\frac{w}{a}\right) - a^2\nabla^2\left(\frac{\Phi}{Ea^2t}\right) - \frac{P}{Et}\left(\frac{\partial^2}{\partial\phi^2} + \tan\phi\,\frac{\partial}{\partial\phi} - \sec^2\phi\,\frac{\partial^2}{\partial\phi^2}\right)\left(\frac{w}{a}\right)\sec^2\phi\right] \times \delta\left(\frac{w}{a}\right)a^2\cos\phi\,d\theta d\phi = 0 \quad (7a)$$

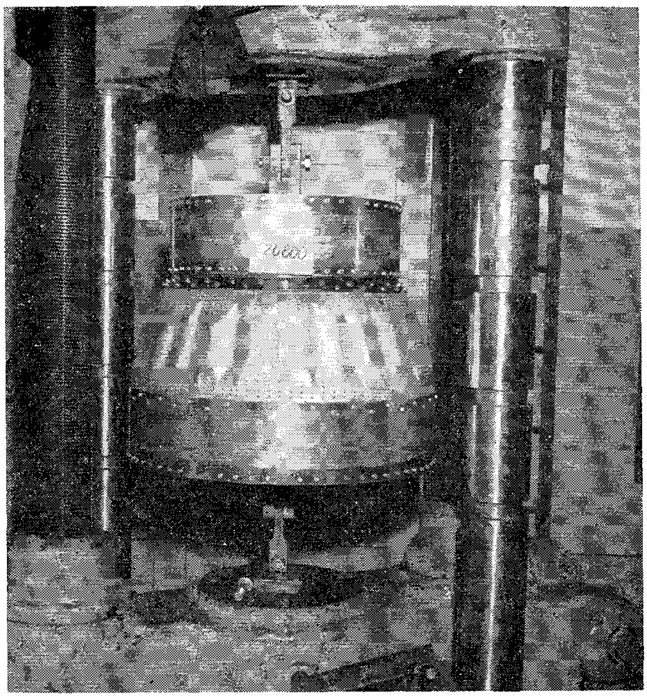

Fig. 1 Truncated hemisphere buckled by axial tension.

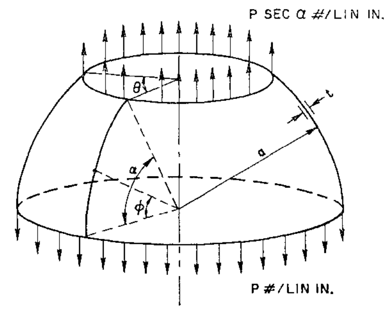

Fig. 2 Shell geometry and load.

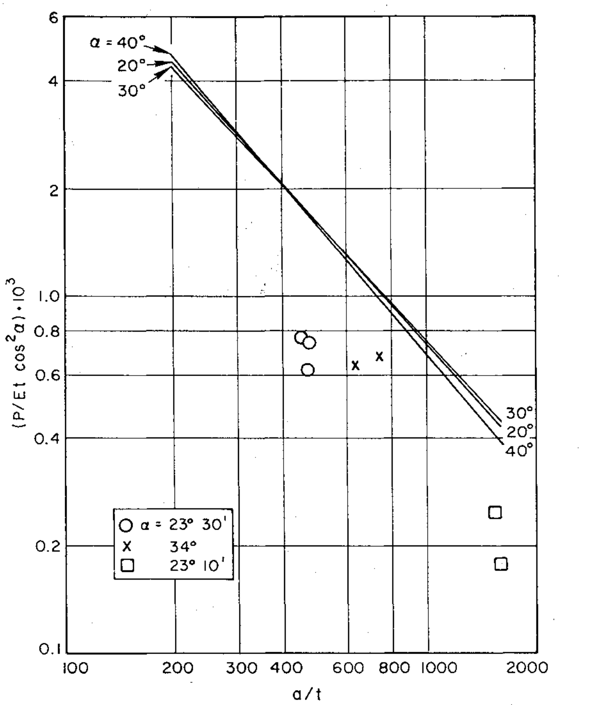

Fig. 3 Buckling stress of truncated hemisphere (μ = 0.3).

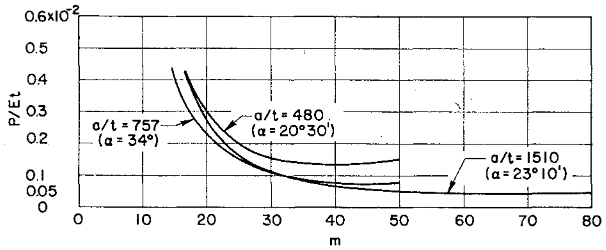

Fig. 4 Buckling forces vs wave numbers.

$$\int_0^\alpha \int_0^{2\pi} \left[a^4\nabla^4\left(\frac{\Phi}{Ea^2t}\right) + a^2\nabla^2\left(\frac{w}{a}\right)\right] \times \delta\left(\frac{\Phi}{Ea^2t}\right) a^2 \cos\phi \, d\theta \, d\phi = 0 \quad (7b)$$

where w and Φ are subjected to the boundary conditions given by Eq. (6b).

For convenience, the following substitutions are introduced:

$$x = \sin\phi \qquad l = \sin\alpha$$
$$\partial/\partial\phi = (1 - x^2)^{1/2}\,(\partial/\partial x), \text{ etc.} \quad (8)$$
$$a^2\nabla^2 = (1-x^2)\frac{\partial^2}{\partial x^2} - 2x\frac{\partial}{\partial x} + \frac{1}{1-x^2}\frac{\partial^2}{\partial\theta^2}$$

The boundary conditions (6b) then become

$$w = \partial w/\partial x = 0 \qquad \text{at } x = 0, l$$
$$\quad (9)$$
$$\Phi = \partial\Phi/\partial x = 0 \qquad \text{at } x = 0, l$$

Suitable expressions for w and Φ which satisfy conditions (9) may be taken as

$$\frac{w}{a} = \sum_{n=2,3,\ldots}^{N} A_n x^n (x-l)^n \cos m\theta$$
$$\quad (10)$$
$$\frac{\Phi}{Ea^2t} = \sum_{n=2,3,\ldots}^{N} B_n x^n (x-l)^n \cos m\theta$$

The substitution of Eqs. (10) into Eq. (7) then leads to

$$\sum_{n=2}^{\infty} (A_n e_{nj} + B_n d_{nj}) = 0$$
$$\sum_{n=2}^{\infty}\left\{\left[\frac{1}{12(1-\mu^2)}\left(\frac{t}{a}\right)^2 d_{nj} - \frac{P}{Et}f_{nj}\right]A_n - B_n e_{nj}\right\} = 0$$
$$j = 2, 3, 4, \ldots N \quad (11)$$

where

$$(-1)^{n+j} d_{nj} = \frac{2(n)^2 (n-1)(n-2)}{(2n+2j-3)!} l^{2n+2j-3} \times \left[\frac{n-3}{n}(n+j)!\,(n+j-4)! - 4\,(n+j-1)! \times (n+j-3)! + 3\,\frac{n-1}{n-2}(n+j-1)!\,(n+j-1)!\right] - \frac{2n\,(n-1)}{(2n+2j-1)!} l^{2n+2j-1}\left\{(7n^2-5n-2)\,(n+j)!\,(n+j-2)! - \left[4n\,(n+1) + \frac{n}{n-1}(6+2m^2)\right][(n+j-1)!]^2 - 4\,(n^2-n-2)(n+j+1)!\,(n+j-3)! + (n-1)(n-2)(n-3)\,(n+j+2)!\,(n+j-4)!\right\} + \frac{n}{(2n+2j+1)!} l^{2n+2j+1}\left\{\left(\frac{m^4-2m^2}{n} + n^3+2n^2+n\right) \times [(n+j)!]^2 - (4n^3+12n^2-14n+4)(n+j+1)! \times (n+j-1)! + (6n^2+18n+14)(n-1)\,(n+j+2)! \times (n+j-2)! - 4\,(n-1)(n^2-4)(n+j+3)! \times (n+j-3)! + (n-1)(n-2)(n-3)(n+j+4)!\,(n+j-4)!\right\} + (2m^4-6m^2)\frac{(n+j)!\,(n+j+2)!}{(2n+2j+3)!} l^{2n+2j+3} + (3m^4-10m^2)\frac{(n+j+4)!\,(n+j)!}{(2n+2j+5)!} l^{2n+2j+5} \quad (12)$$

$$(-1)^{n+j} e_{nj} = \frac{2n}{(2n+2j-1)!} l^{2n+2j-1}\left\{(n-1)(n+j)! \times (n+j-2)! - n\,[(n+j-1)!]^2\right\} - \frac{n}{(2n+2j+1)!} \times l^{2n+2j+1}\left\{\left(n+1 + \frac{m^2}{n}\right)[(n+j)!]^2 - 2(n+1)(n+j+1)!\,(n+j-1)! + (n-1)(n+j+2)! \times (n+j-2)!\right\} - m^2\frac{(n+j+2)!\,(n+j)!}{(2n+2j+3)!} l^{2n+2j+3} - m^2\frac{(n+j)!\,(n+j+4)!}{(2n+2j+5)!} l^{2n+2j+15} \quad (13)$$

$$(-1)^{n+j} f_{nj} = \frac{2n}{(2n+2j-1)!} l^{2n+2j-1}\left\{(n-1)(n+j)! \times (n+j\text{-}2)! - n\,[(n+j-1)!]^2\right\} + m^2\frac{[(n+j)!]^2}{(2n+2j+1)!} \times l^{2n+2j+1} + m^2 \times \frac{(n+j+2)!\,(n+j)!}{(2n+2j+3)!} l^{2n+2j+3} + m^2\frac{(n+j+4)!\,(n+j)!}{(2n+2j+5)!} l^{2n+2j+5} \quad (14)$$

For a nontrivial solution for A_n and B_n, the determinant of their coefficients in Eqs. (11) must vanish, yielding the stability criterion for the problem. The lowest root of the determinal equation is the critical value of the load parameter P/Et.

Table 1 Comparison of experimental and theoretical results

				P/tE (theory)				
$\frac{P}{Et\cos^2\alpha} \times 10^3$	α	a/t	P/tE (test)	1st approx.	2nd approx.	3rd approx.	4th approx.	Number of circumferential waves
0.73	23°30′	480	6.15×10^{-4}	13.5945×10^{-4}	13.5528×10^{-4}	13.4911×10^{-4}	13.4903	40
0.62		476	5.18	13.7227	13.6806	13.6185	13.6177	40
0.79		455	6.60	14.4167	14.3617	14.2942	14.2936	38
0.68	34°	757	4.72	7.70351	7.53251	7.28196	7.05160	48
0.64		637	4.38	9.21024	9.04707	8.78546	8.56413	44
0.18	23°10′	1600	1.47	3.82673	3.82654	3.80973	3.80557	72
0.25		1510	2.06	4.06189	4.06182	4.04427		70

III. Numerical Results and Discussion

Computations for the buckling tension load were carried out for shells with $\alpha = 20°$, $30°$, and $40°$ and a/t ranging from 200 to 1600. Four terms each were used in the summation of Eqs. (10). The output is given by the nondimensional quantity $P/Et \cos^2\alpha$ against a/t as shown in Fig. 3. It may be seen that, within the range of α (that is, α is less than 40°), the buckling strength of the shell is influenced far less by α than by a/t. The curve shown in Fig. 3 also may be expressed by the following approximate formula:

$$P/Et \cos^2\alpha = 1.57\ (t/a)^{1.12} \tag{15}$$

In the limiting case where the radius of the sphere approaches infinity, the problem is reduced to a narrow, infinitely long strip that is subjected to compression along the length and tension across the width of the strip. In this case, the buckling stress is of the form (Ref. 3, p. 337)

$$P/Et = k\ (t/a\alpha)^2 \tag{16}$$

where k is a constant coefficient.

One recalls (Ref. 3, pp. 478, 517) that the classical buckling stress for cylindrical shells under radial pressure is

$$\frac{\sigma_{cr}}{E} = \frac{1}{4\ (1-\mu^2)} \left(\frac{t}{a}\right)^2 \tag{17}$$

and that the classical buckling stress for spherical shells under external pressure is

$$\frac{\sigma_{cr}}{E} = \frac{1}{[3(1-\mu^2)]^{1/2}} \left(\frac{t}{a}\right) \tag{18}$$

One may see from Eqs. (4) and (15) that the buckling characteristic of the present problem is similar to the sphere problem rather than the cylinder problem.

Test data for five samples of various geometry were furnished by Douglas Aircraft Company and are reproduced here in Table 1. The theoretical buckling load parameter P/Et obtained by using one term in the summation of Eq. (10) as the first approximation and succeedingly using more terms in the summation as higher approximations also is shown. Note that the convergence of the series solution is good and that using four terms in the summation is adequate for practical purposes. The theoretical values are found to be about twice greater than the experimental values, a difference rather common in buckling problems. Also given in Table 1 are the theoretical circumferential buckling wave numbers associated with the found theoretical minimum buckling loads. These numbers seem quite high in comparion with the wave numbers found by test. However, a study of the curves for the theoretical buckling load vs wave numbers in Fig. 4 leads to the belief that the actual buckling wave number probably is determined by the initial imperfection of the shell, since the curve in the neighborhood of the theoretical minimum point is rather flat.

The subject problem is an interesting one, as it is a particular example that an elastic system is buckled by tension, although the real cause of the instability is the compressive hoop stress. Certainly, there remain many areas for future studies, among them determination of the buckling load by large deflection theory and consideration of initial imperfections. The testing results presented here are rather scarce and scattered, hardly enough to give any conclusive indication. Extensive and systematic experiments in this respect are recommended.

References

[1] Novozhilov, V. V., *The Theory of Thin Shells*, transl. from Russian by P. G. Lowe (P. Noordhoff, Netherlands, 1959), p. 87.

[2] Galerkin, B. G., "Series solutions of some problems of elastic equilibrium of rods and plates," Vestn. Inzh. i Tekhn. **1**, 879–908 (1915); also Wang, C.-J., *Applied Elasticity*, (McGraw-Hill Book Co. Inc., New York, 1953), p. 162.

[3] Timoshenko, S. and Gere, J. M., *Theory of Elastic Stability* (McGraw-Hill Book Co. Inc., New York, 1961), pp. 478, 517.